Fermi National Accelerator Laboratory,
P.O. Box 500, Batavia, IL, 60510

TD-05-054
12/13/2005

Magnetic analysis of 3 and 4-layer dipole magnets

V.V. Kashikhin, A.V. Zlobin

I. Introduction

Fermilab superconducting magnet group has been working on Nb_3Sn accelerator magnet technology development exploring different superconducting strands and design concepts. Several short dipole models built with the MJR conductor reached the quench currents on a level of 50-60% of the short sample limit. The reason of poor quench performance was identified and associated with the magnetic instabilities in superconducting strands. In order to experimentally confirm the theoretical findings of the magnetic instability model and demonstrate viability of the magnet mechanical structure, a short dipole model based on more stable PIT conductor but identical to the previous models coil geometry and mechanical structure has been fabricated and tested and reached its short sample limit of 10 T after a moderate training.

Moving towards higher fields is the next logical step in the magnet development for exploring the limits of A15 superconductors and addressing the DOE quest for high fields in accelerator-relevant magnets. The PIT conductor would be a preferable choice in terms of the magnet stability; however it lacks the critical current density (J_c(12T, 4.2K) ~ 2000 A/mm^2) necessary to achieve the high fields and is more sensitive to mechanical stresses than other conductors. The RRP conductor on the other hand offers the highest critical current density (J_c(12T, 4.2K) ~ 3000 A/mm^2) and lower sensitivity to mechanical stress, but is unstable at low fields. A newly emerging Nb_3Al conductor has critical current density and stability characteristics similar to PIT, but is mechanically superior to any other A15 conductor.

These considerations need to be carefully taken into account during the magnet design process. The purpose of this note is to overview the possible dipole magnet designs that can potentially achieve higher fields based on the present understanding of the conductor behavior and require minimum resources for fabrication at Fermilab by reutilizing as much of the available tooling and equipment as possible.

II. Magnets using HFDA/TQ2a/CC tooling

MJR and RRP are the only Nb_3Sn conductors on the market today able to carry enough current density to achieve high fields at relatively high stresses. Also in part due to this ability they are not stable enough at low fields that was confirmed both theoretically and experimentally on HFDA and HFDM models made of 1-mm MJR and 0.7-mm RRP strands [1]-[3]. Thus to realize the MJR and RRP conductor potential and avoid the stability issues one needs to limit the use of these conductors to the cases where the actual J_c(B) characteristic has a negative slope[1] that corresponds to the field region above ~3 T [4].

[1] This is a simplified stability criterion that however for these particular conductors is close to the general stability criterion.

It is clear that this requirement can not be fulfilled in a 2-layer shell type magnet with the same cable in the inner and outer layers as there always is a low field region in the outer layer. Thus, for achieving higher fields it is necessary to increase the number of layers. In this regard, the most cost effective and fast way towards higher fields is to choose such layer dimensions that the inner layers fit the HFDA production tooling with the maximum outer radius of 52.0 mm and the outermost layer(s) fit(s) the TQ2a production tooling with the maximum outer radius of 68.2 mm.

a) 3-layer magnet based on 1-mm PIT strand

The first idea was to use the existing HFDA 28-strand cable and add one layer on top of the HFDA coil. To achieve a good field quality and have relatively simple coil geometry it was necessary to re-optimize the inner two layers. However, during the optimization it was possible to remove one wedge from the middle layer while retaining the good field quality. Thus the number of end-parts is the same as in HFDA magnets.

The coil and yoke geometry with the flux density plots are shown in Figures 1-2 and the cable and magnet parameters are summarized in Tables 1-3. The peak field point that defines the magnet performance belongs to the pole turn of the inner layer. If the coil is wound without splices (i.e. the same cable in all the layers) then the only stable enough candidate is the PIT conductor that limits the quench bore field at 13.2 T and the peak coil field at 13.8 T. At this field level the coil stress reach 101 MPa that is comparable with the stresses in HFDA05 magnet.

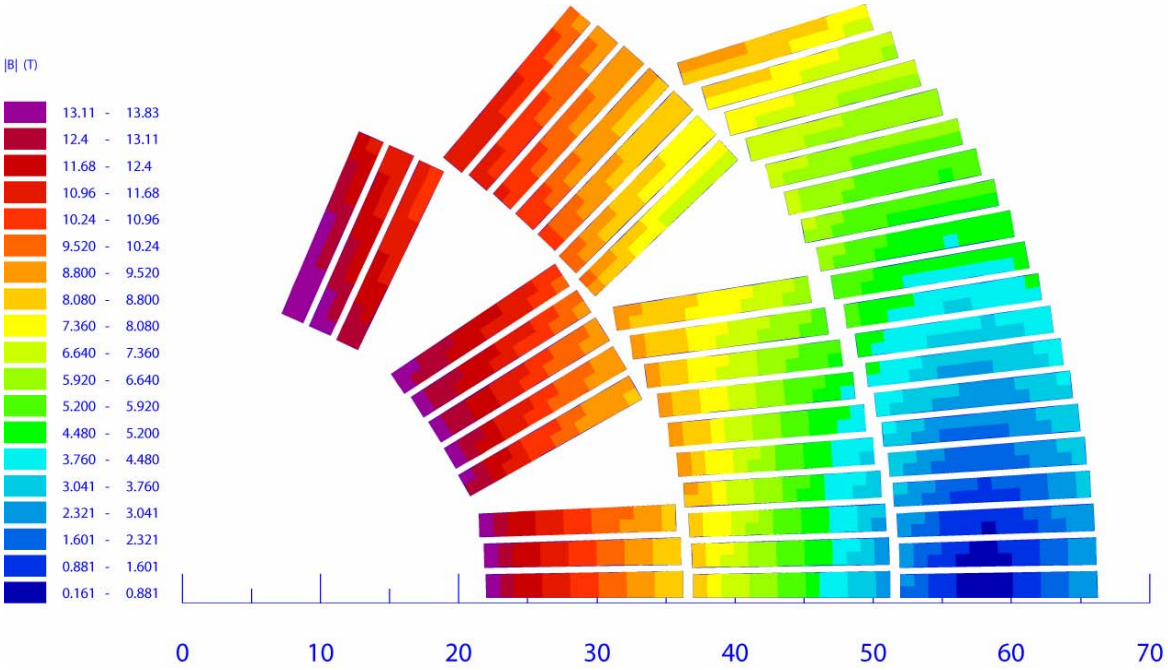

Figure 1. Flux density in the coil cross-section.

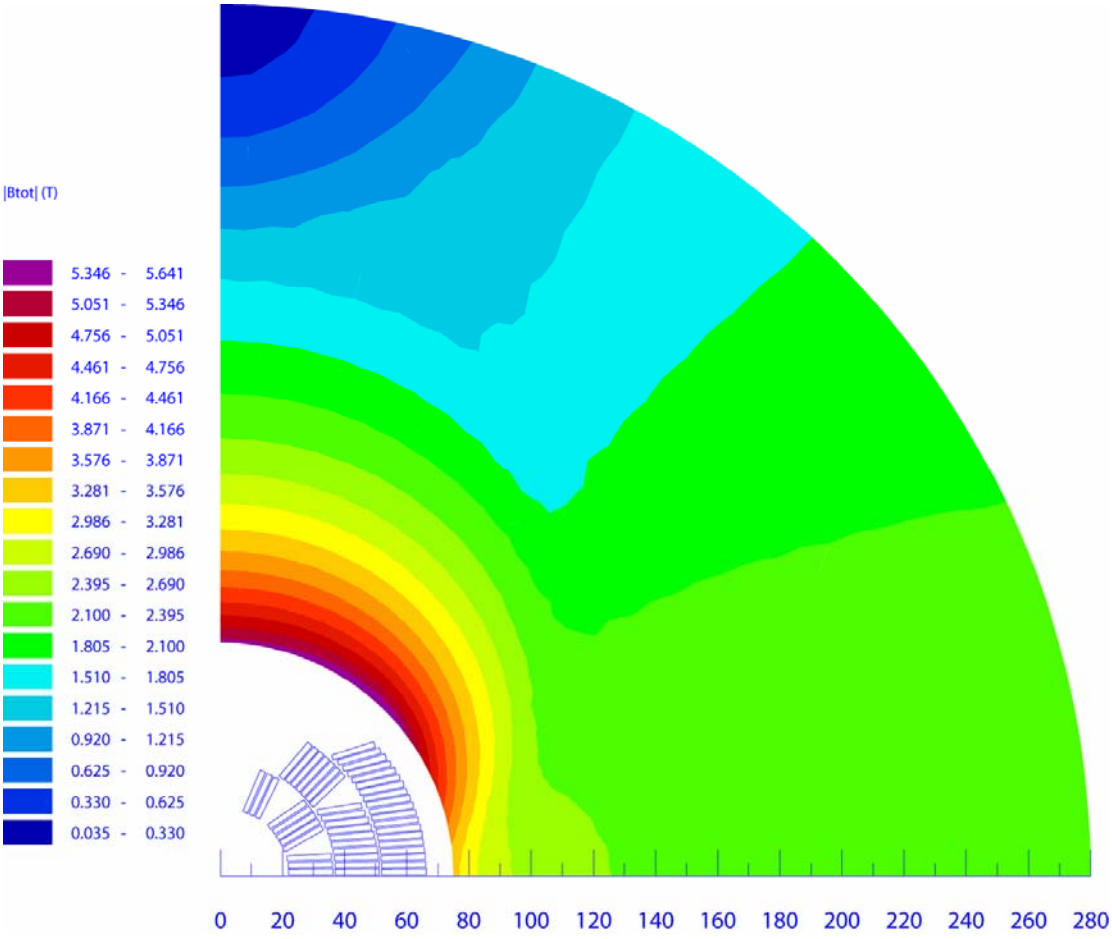

Figure 2. Flux density in the yoke cross-section.

Table 1. Cable parameters.

Parameter	Unit	Inner coil
N of strands	-	**28**
Strand diameter	mm	**1.000**
Bare cable width	mm	**14.232**
Bare inner cable edge thickness	mm	**1.687**
Bare outer cable edge thickness	mm	**1.913**
Cabling angle	deg.	**14.5**
Radial insulation thickness	mm	**0.254**
Azimuthal insulation thickness	mm	**0.254**
Copper to non-copper ratio	-	**1.000**

Table 2. Systematic field harmonics at $R_{bore}/2$ radius.

n	b_n, 10^{-4}	
	I=1kA	$I=I_{quench}$
3	0.00028	-1.19239
5	0.00098	0.06307
7	0.00299	0.00385
9	-0.01463	-0.01638
11	0.06362	0.07126
13	-0.00236	-0.00265

Table 3. Magnet parameters.

Parameter	Unit	Value
N of layers		**3**
N of turns in the inner coil		**56**
N of turns in the outer coil		**38**
Total coil area (Cu + nonCu)	cm^2	**42.70**
Assumed non-Cu J_c at 12 T, 4.2 K	A/mm^2	**2000**
Bore quench field	T	**13.24**
Quench current	kA	**14.86**
Peak field in the inner coil at quench	T	**13.84**
Peak field in the outer coil at quench	T	**9.04**
Inner coil margin at quench	%	**0.00**
Outer coil margin at quench	%	**26.89**
Magnet inductance at quench	mH/m	**5.07**
Stored energy at quench	kJ/m	**559.78**
Horizontal Lorentz force/I quadrant at quench	MN/m	**4.01**
Vertical Lorentz force/I quadrant at quench	MN/m	**-1.93**
Midplane pressure in the inner coil at quench	MPa	**101**
Midplane pressure in the outer coil at quench	MPa	**79**

b) 4-layer magnet based on 1-mm MJR(RRP)/Nb_3Al strands

The maximum field in the magnet design presented in the previous paragraph was limited at 13.2 T field due to the inability to use high-Jc conductors in the coils made of a single piece of cable. Thus a 4-layer design with the different cables in the inner and outer layers was considered.

The coil and yoke geometry with the flux density plots are shown in Figures 3-4 and the cable and magnet parameters are summarized in Tables 4-6. The inner coil is identical to the HFDA type coils. The outer coil is made of twice narrower cable using the same strand that grades the current density between the inner and the outer layers by a factor of two. The quench bore field of 14.1 T is limited by the outer coil layers for the same critical current density in all the layers. As a consequence, this design can not benefit from using RRP conductor in the inner layers (that however is acceptable in terms of the magnet stability), though the quench field is ~1 T higher than in 3-layer design thanks to the grading.

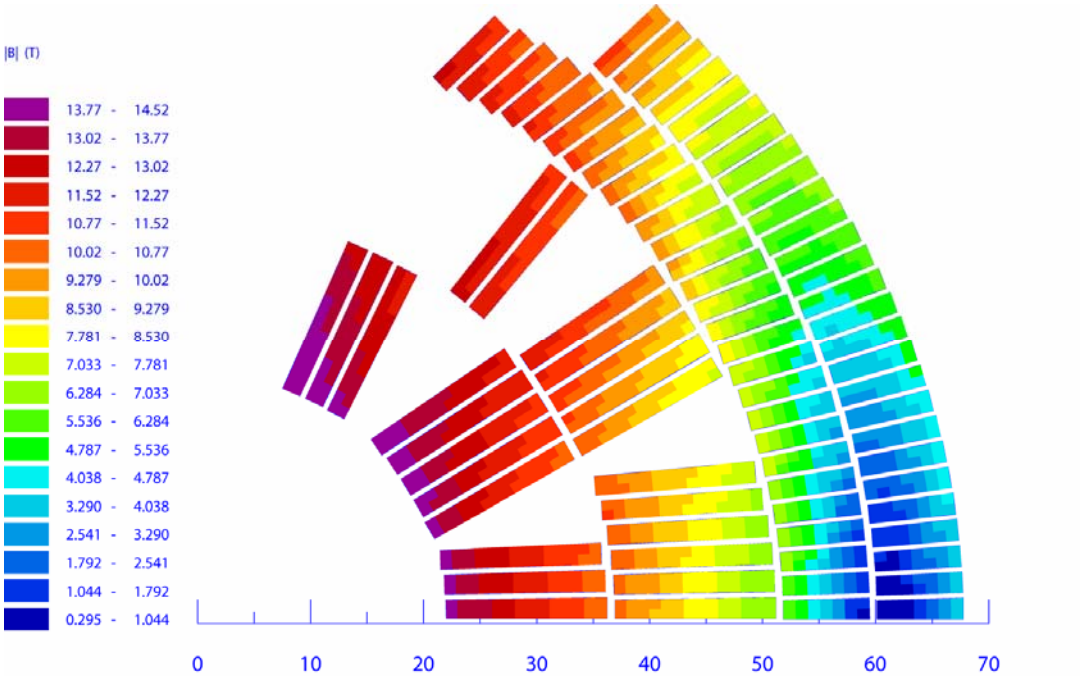

Figure 3. Flux density in the coil cross-section.

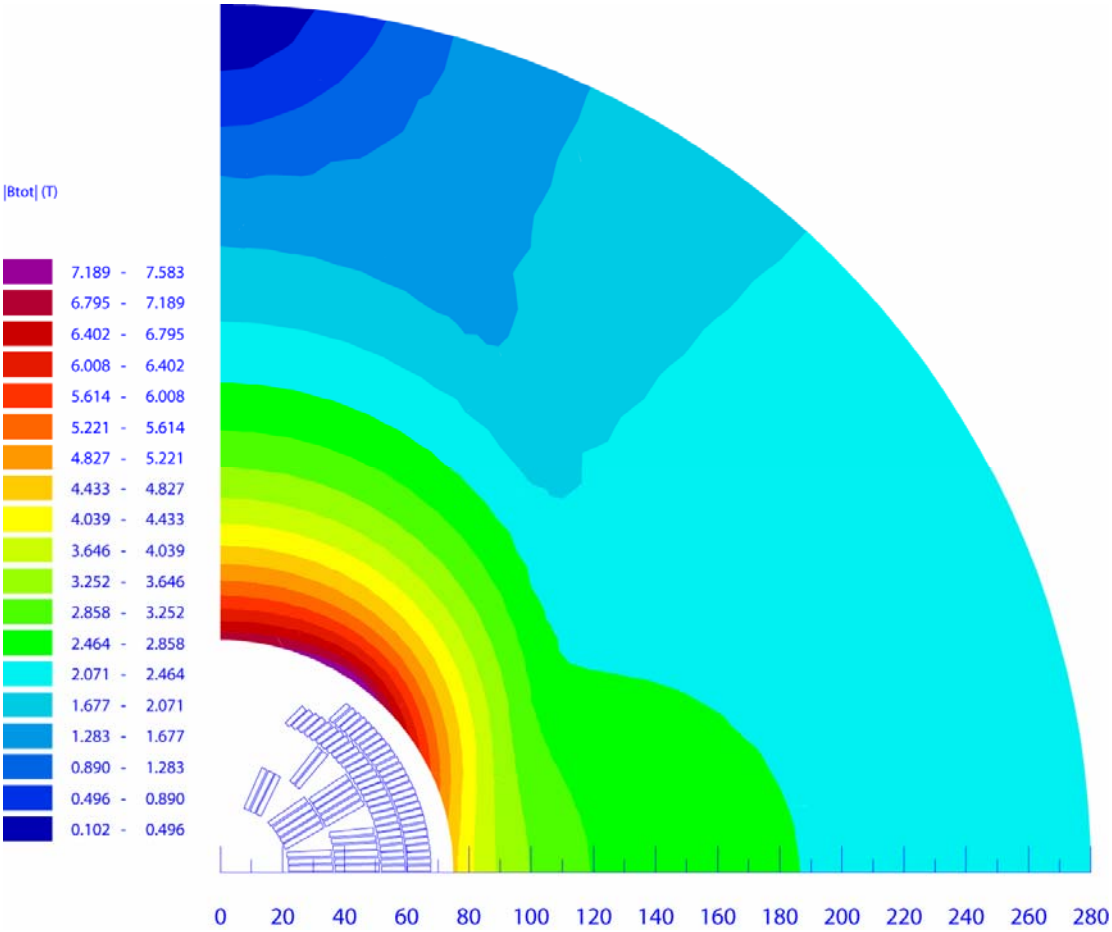

Figure 4. Flux density in the yoke cross-section.

Table 4. Cable parameters.

Parameter	Unit	Inner coil	Outer coil
N of strands	-	**28**	**15**
Strand diameter	mm	**1.000**	**1.000**
Bare cable width	mm	**14.232**	**7.635**
Bare inner cable edge thickness	mm	**1.687**	**1.669**
Bare outer cable edge thickness	mm	**1.913**	**1.882**
Cabling angle	deg.	**14.5**	**14.5**
Radial insulation thickness	mm	**0.254**	**0.225**
Azimuthal insulation thickness	mm	**0.254**	**0.225**
Copper to non-copper ratio	-	**1.000**	**1.000**

Table 5. Systematic field harmonics at $R_{bore}/2$ radius.

n	b_n, 10^{-4}	
	I=1kA	$I=I_{quench}$
3	-1.0754	0.13626
5	-0.6008	-0.63001
7	0.0122	0.01443
9	-0.0359	-0.04327
11	0.0391	0.04706
13	-0.0007	-0.00081

Table 6. Magnet parameters.

Parameter	Unit	Value
N of layers		**4**
N of turns in the inner coil		**48**
N of turns in the outer coil		**110**
Total coil area (Cu + nonCu)	cm^2	**48.58**
Assumed $J_c^{non\text{-}Cu}$(12 T, 4.2 K)	A/mm^2	**2000**
Bore quench field	T	**14.08**
Quench current	kA	**10.92**
Peak field in the inner coil at quench	T	**15.06**
Peak field in the outer coil at quench	T	**12.37**
Inner coil margin at quench	%	**3.62**
Outer coil margin at quench	%	**0.00**
Magnet inductance at quench	mH/m	**13.99**
Stored energy at quench	kJ/m	**834.13**
Horizontal Lorentz force/I quadrant at quench	MN/m	**5.21**
Vertical Lorentz force/I quadrant at quench	MN/m	**-2.47**
Midplane pressure in the inner coil at quench	MPa	**61.6**
Midplane pressure in the outer coil at quench	MPa	**242.6**

Due to the twice narrower cable, the midplane pressure in the outer layers reach a whooping 243 MPa that is way above the tolerable pressure for Nb_3Sn conductor thus leaving the Nb_3Al conductor as the only feasible option for the outer layers.

c) 4-layer magnet based on 1-mm MJR(RRP)/PIT strands

To accommodate the more pressure-sensitive Nb3Sn conductors for the 4-layer magnet design presented earlier, a number of turns was removed from the outer layers.

The coil and yoke geometry with the flux density plots are shown in Figures 5-6 and the cable and magnet parameters are summarized in Tables 7-9. Removing the turns heavily impacted the field quality with 65 units of the sextupole component as well as the bore quench field that dropped to 13.5 T – that is just 0.3 T higher than the quench field of the 3-layer magnet.

Similarly to the previous design, the magnet performance is limited by the outer layers for the same critical current density in all the layers. The midplane pressure was reduced below the "magic" for a Nb_3Sn conductor value of 150 MPa, though may still be too large for the highly pressure-sensitive PIT conductor.

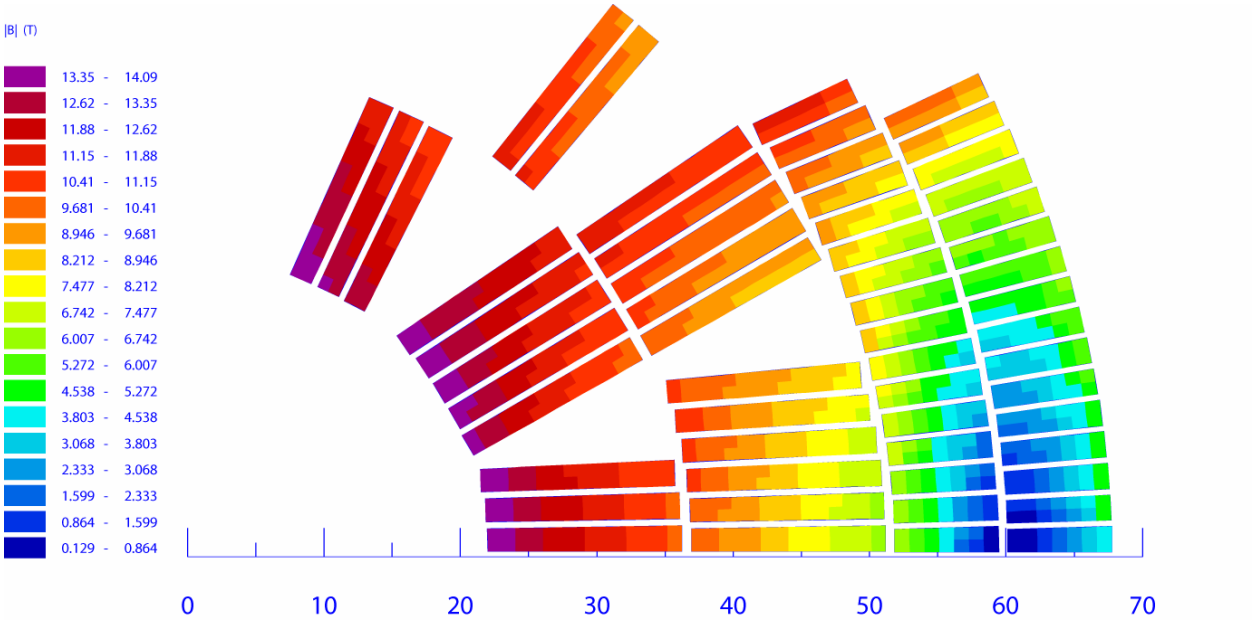

Figure 5. Flux density in the coil cross-section.

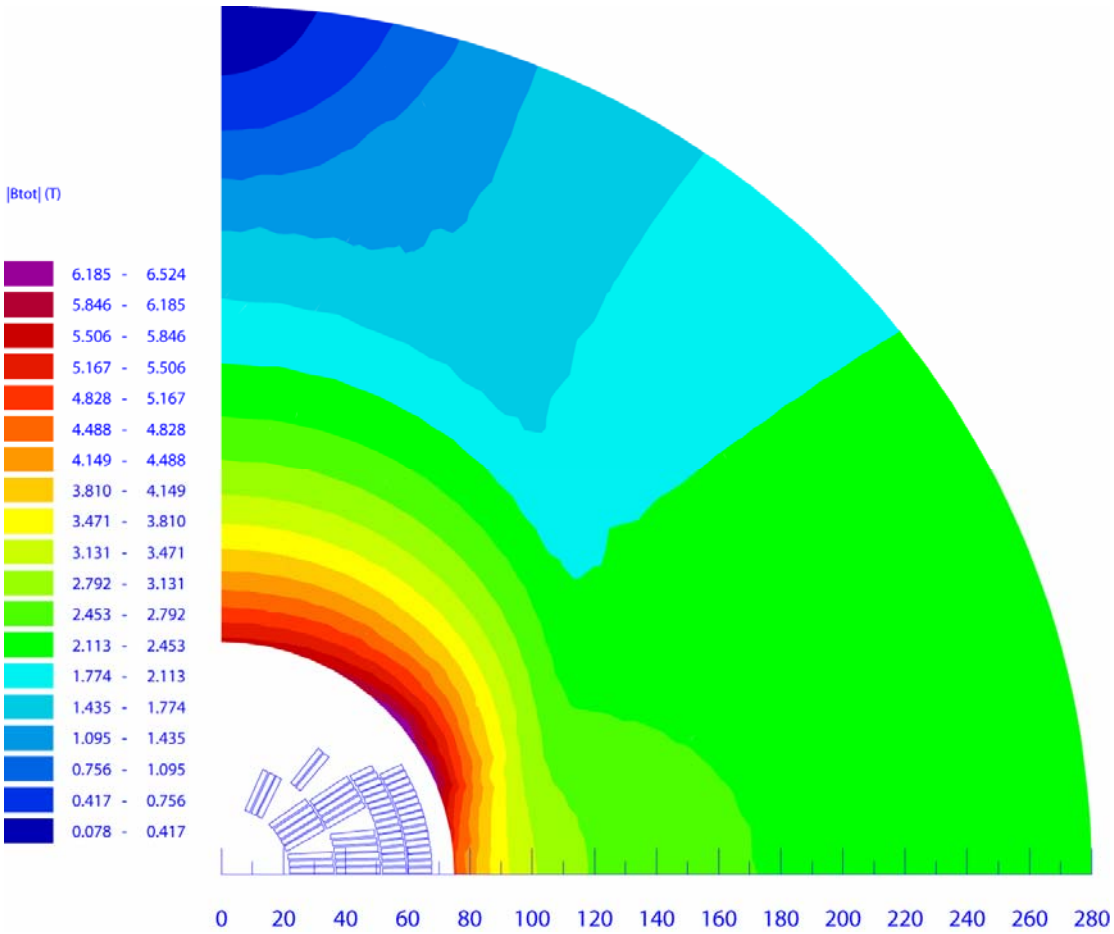

Figure 6. Flux density in the yoke cross-section.

Table 7. Cable parameters.

Parameter	Unit	Inner coil	Outer coil
N of strands	-	**28**	**15**
Strand diameter	mm	**1.000**	**1.000**
Bare cable width	mm	**14.232**	**7.635**
Bare inner cable edge thickness	mm	**1.687**	**1.669**
Bare outer cable edge thickness	mm	**1.913**	**1.882**
Cabling angle	deg.	**14.5**	**14.5**
Radial insulation thickness	mm	**0.254**	**0.225**
Azimuthal insulation thickness	mm	**0.254**	**0.225**
Copper to non-copper ratio	-	**1.000**	**1.000**

Table 8. Systematic field harmonics at $R_{bore}/2$ radius.

n	b_n, 10^{-4}	
	I=1kA	$I=I_{quench}$
3	65.3208	65.2674
5	0.0868	0.1083
7	-0.0194	-0.0217
9	-0.0460	-0.0538
11	0.0500	0.0584
13	-0.0009	-0.0010

Table 9. Magnet parameters.

Parameter	Unit	Value
N of layers		**3**
N of turns in the inner coil		**48**
N of turns in the outer coil		**64**
Total coil area (Cu + nonCu)	cm^2	**37.38**
Assumed non-Cu J_c at 12 T, 4.2 K	A/mm^2	**2000**
Bore quench field	T	**13.53**
Quench current	kA	**13.02**
Peak field in the inner coil at quench	T	**14.35**
Peak field in the outer coil at quench	T	**11.47**
Inner coil margin at quench	%	**1.82**
Outer coil margin at quench	%	**0.00**
Magnet inductance at quench	mH/m	**8.33**
Stored energy at quench	kJ/m	**706.05**
Horizontal Lorentz force/I quadrant at quench	MN/m	**4.17**
Vertical Lorentz force/I quadrant at quench	MN/m	**-2.50**
Midplane pressure in the inner coil at quench	MPa	**74**
Midplane pressure in the outer coil at quench	MPa	**146**

III. Magnets partially using HFDA/TQ2a/CC tooling

The magnet designs presented in the previous section made the maximum use of the available tooling. However, it is clear that these designs can not fully unfold the potential of the RRP conductor as with the tooling-defined layer radii they are limited by the conductor performance in the outer layer(s). Thus a redistribution of the cable width was necessary to charge the inner coil layers with the RRP current density.

a*) 4-layer magnet fitting TQ2a tooling based on 1-mm RRP/PIT(Nb_3Al) strands*

The coil aperture of this magnet was chosen the same as in HFDA magnets and the coil outer diameter was chosen to fit the TQ2a tooling. The cable size was optimized to fill the space between these two constrains in a 4-layer configuration. In this case at least the HFDA winding mandrel and TQ2a curing, reaction and impregnation fixtures can be used without changes. The coil and yoke geometry with the flux density plots are shown in Figures 7-8 and the cable and magnet parameters are summarized in Tables 10-12.

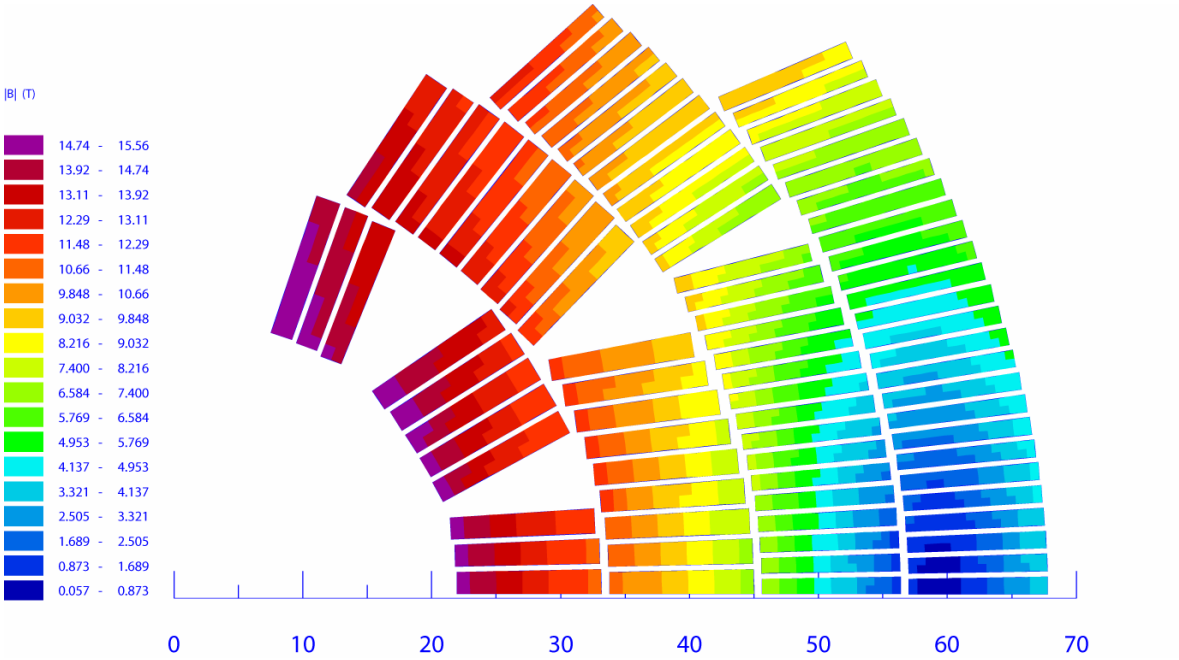

Figure 7. Flux density in the coil cross-section.

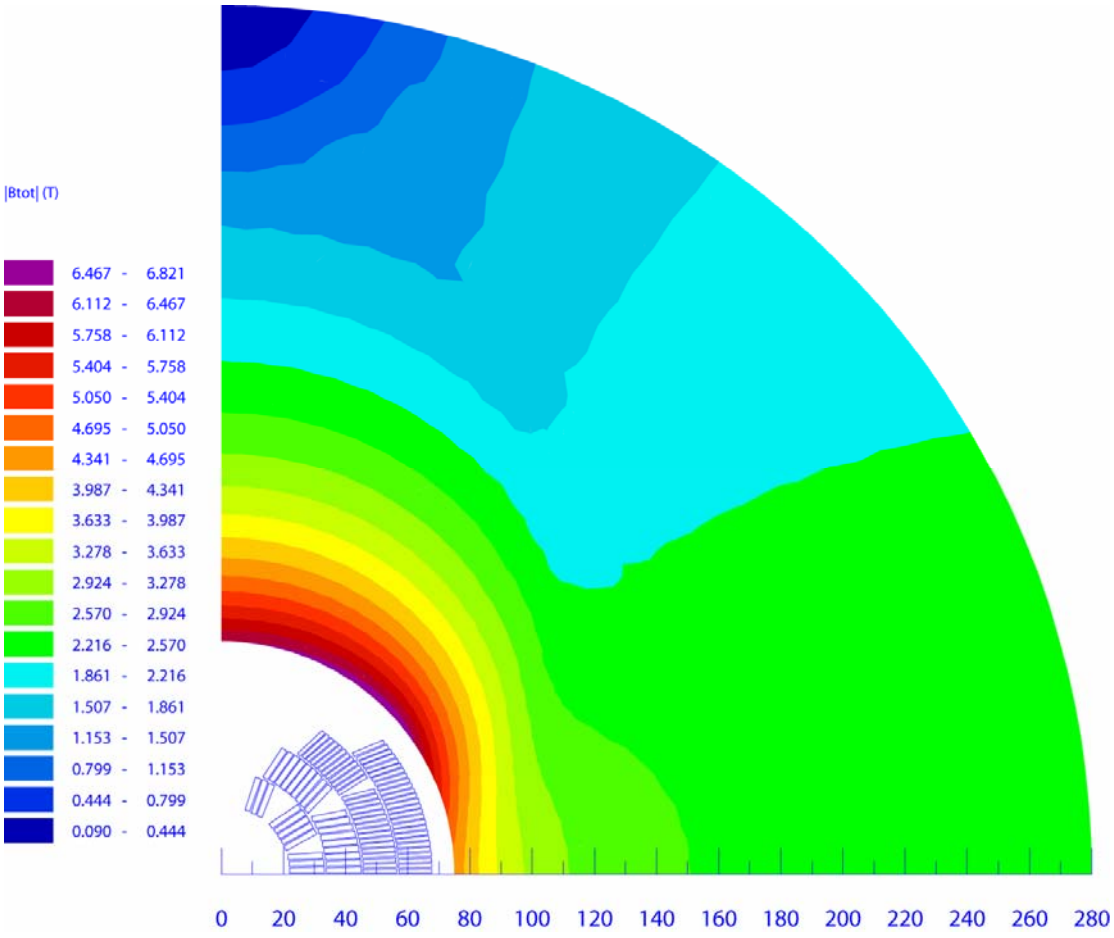

Figure 8. Flux density in the yoke cross-section.

Table 10. Cable parameters.

Parameter	Unit	Inner coil	Outer coil
N of strands	-	**22**	**30**
Strand diameter	mm	**1.000**	**0.700**
Bare cable width	mm	**11.183**	**10.742**
Bare inner cable edge thickness	mm	**1.676**	**1.165**
Bare outer cable edge thickness	mm	**1.910**	**1.333**
Cabling angle	deg.	**14.5**	**14.5**
Radial insulation thickness	mm	**0.225**	**0.225**
Azimuthal insulation thickness	mm	**0.225**	**0.225**
Copper to non-copper ratio	-	**1.000**	**1.000**

Table 11. Systematic field harmonics at $R_{bore}/2$ radius.

n	b_n, 10^{-4}	
	I=1kA	$I=I_{quench}$
3	0.0003	-3.6583
5	-0.0008	0.0556
7	-0.0043	-0.0046
9	-0.0307	-0.0360
11	0.0489	0.0574
13	-0.0011	-0.0013

Table 12. Magnet parameters.

Parameter	Unit	Value
N of layers		**4**
N of turns in the inner coil		**58**
N of turns in the outer coil		**108**
Total coil area (Cu + nonCu)	cm^2	**44.46**
Assumed non-Cu J_c at 12 T, 4.2 K in the inner coil	A/mm^2	**2800**
Assumed non-Cu J_c at 12 T, 4.2 K in the outer coil	A/mm^2	**2000**
Bore quench field	T	**14.98**
Quench current	kA	**10.27**
Peak field in the inner coil at quench	T	**15.81**
Peak field in the outer coil at quench	T	**12.58**
Inner coil margin at quench	%	**1.59**
Outer coil margin at quench	%	**0.00**
Magnet inductance at quench	mH/m	**15.54**
Stored energy at quench	kJ/m	**819.52**
Horizontal Lorentz force/I quadrant at quench	MN/m	**5.39**
Vertical Lorentz force/I quadrant at quench	MN/m	**-2.70**
Midplane pressure in the inner coil at quench	MPa	**156.6**
Midplane pressure in the outer coil at quench	MPa	**125.7**

Due to the cable width redistribution it is possible to use (and benefit from) the RRP conductor in the inner layers while using the lower-Jc PIT or Nb_3Al conductors in the outer layers. With these conductors the magnet would reach the bore quench field of 15.0 T, while the midplane pressures are within reasonable limits of 157 MPa for the inner layers and 126 MPa for the outer layers.

It is interesting to compare parameters of this magnet with the parameters of 15-T block type magnet based on the RRP conductor with the same characteristics [5]. While the coil of the block type design may look more compacted due to absence of the angle-compensating wedges, it reaches the same quench field in 24% smaller useful aperture at 31 % larger conductor area and 15 % higher stresses under full excitation. Moreover, since the block-type coil uses the same high-Jc strand everywhere, including the low-field regions, this magnet is potentially unstable that depending on the strand RRR may or may not reach the designed field. This comparison clearly demonstrates the advantages of the shell-type coils over the block-type designs.

b*) 4-layer magnet not-fitting TQ2a tooling based on 1-mm RRP/PIT(Nb_3Al) strands*

The 4-layer magnet design presented in the previous paragraph was optimized to fit the TQ2a tooling that required new (or modified) winding and curing tooling for all but the outermost layer. Another possibility is to use the unchanged HFDA winding, curing, reaction and impregnation tooling for the inner layers similarly to the 4-layer designs described in the previous section, but add the outer layers of the same thickness. Obviously, it will require all new tooling for the outer layers.

The coil and yoke geometry with the flux density plots are shown in Figures 9-10 and the cable and magnet parameters are summarized in Tables 13-15.

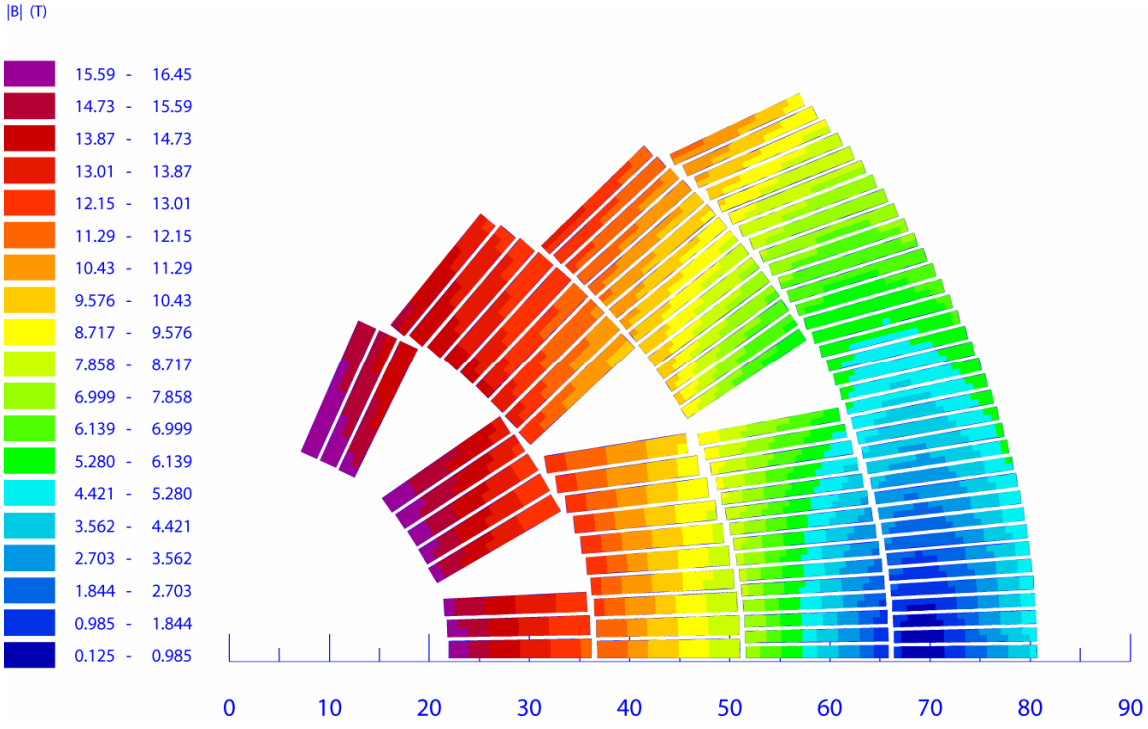

Figure 9. Flux density in the coil cross-section.

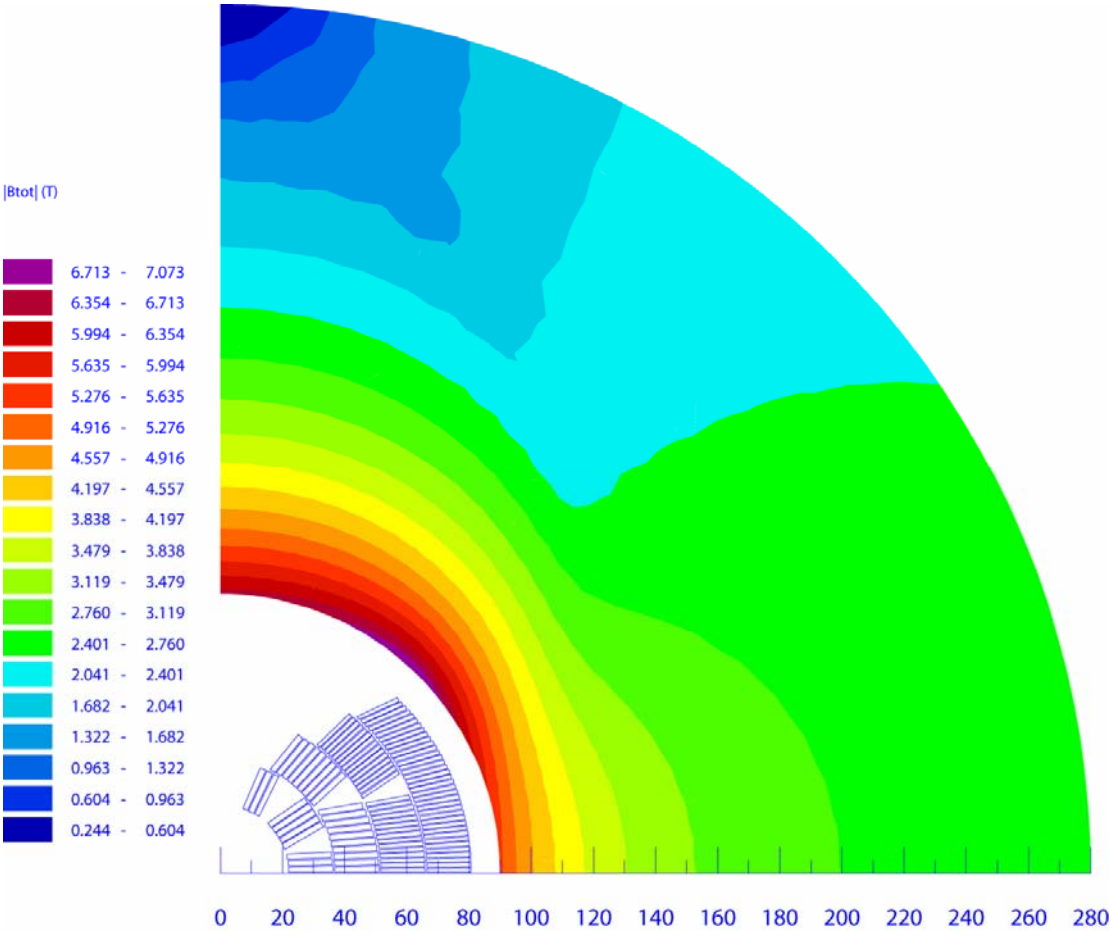

Figure 10. Flux density in the yoke cross-section.

Table 13. Cable parameters.

Parameter	Unit	Inner coil	Outer coil
N of strands	-	**28**	**39**
Strand diameter	mm	**1.000**	**0.700**
Bare cable width	mm	**14.232**	**14.232**
Bare inner cable edge thickness	mm	**1.687**	**1.140**
Bare outer cable edge thickness	mm	**1.913**	**1.314**
Cabling angle	deg.	**14.5**	**14.5**
Radial insulation thickness	mm	**0.200**	**0.200**
Azimuthal insulation thickness	mm	**0.200**	**0.200**
Copper to non-copper ratio	-	**1.000**	**1.000**

Table 14. Systematic field harmonics at $R_{bore}/2$ radius.

n	b_n, 10^{-4}	
	I=1kA	$I=I_{quench}$
3	0.0001	-3.3333
5	0.0002	0.0273
7	0.0019	0.0024
9	0.0022	0.0026
11	0.0441	0.0526
13	-0.0013	-0.0015

Table 15. Magnet parameters

Parameter	Unit	Value
N of layers		**4**
N of turns in the inner coil		**60**
N of turns in the outer coil		**132**
Total coil area (Cu + nonCu)	cm^2	**68.18**
Assumed non-Cu J_c at 12 T, 4.2 K in the inner coil	A/mm^2	**2800**
Assumed non-Cu J_c at 12 T, 4.2 K in the outer coil	A/mm^2	**2000**
Bore quench field	T	**15.96**
Quench current	kA	**11.22**
Peak field in the inner coil at quench	T	**16.45**
Peak field in the outer coil at quench	T	**13.37**
Inner coil margin at quench	%	**0.00**
Outer coil margin at quench	%	**0.90**
Magnet inductance at quench	mH/m	**20.04**
Stored energy at quench	kJ/m	**1261.40**
Horizontal Lorentz force/I quadrant at quench	MN/m	**6.74**
Vertical Lorentz force/I quadrant at quench	MN/m	**-3.57**
Midplane pressure in the inner coil at quench	MPa	**111.8**
Midplane pressure in the outer coil at quench	MPa	**143.0**

Similarly to the previous design, it was possible to grade the inner and outer layers such that the inner layers use the maximum performance of the RRP conductor and the outer layers use stable PIT or Nb_3Al conductor. The magnet reaches the quench bore field of 16.0 T at a moderate midplane pressure of 112 MPa in the inner layers and high but tolerable pressure of 143 MPa in the outer layers.

IV. CONCLUSION

Different magnetic designs of the shell-type magnets that can be made using available HFDA/TQ2a/CC tooling were developed. Depending on the amount of available tooling used and possibility of modifying old or acquiring new tooling, the magnets can reach 13.2-16.0 T fields.

It was shown that in the case of complete adoption of HFDA/TQ2a tooling the magnets are limited by the conductor performance in the outer layers and can reach a maximum of 13.5 T field.

Dropping the requirement of the intermediate layers to match the existing tooling offers more flexibility in choosing the layer dimensions that is beneficial for achieving fields up to 16.0 T.

A comparison between shell and block-type coils with the same quench field demonstrated that the shell-type coil is more effective than the block-type in terms of the coil aperture, conductor area and maximum stress under excitation.

REFERENCES

1. A.V. Zlobin, G. Ambrosio, N. Andreev, E. Barzi, B. Bordini, R. Bossert, R. Carcagno, D.R. Chichili, J. DiMarco, L. Elementi, S. Feher, V.S. Kashikhin, V.V. Kashikhin, R. Kephart, M.J. Lamm, P.J. Limon, I. Novitski, D. Orris, Y. Pischalnikov, P. Schlabach, R. Stanek, J. Strait, C. Sylvester, M. Tartaglia, J.C. Tompkins, D. Turrioni, G. Velev, R. Yamada, V. Yarba, **"R&D of Nb_3Sn Accelerator Magnets at Fermilab"**, *IEEE Transactions on Applied Superconductivity, Vol. 15, No. 2, June 2005, pp.1113-1118.*
2. S. Feher, **"HFDM 04 Test Summary Report"**, Fermilab note, TD-05-030.
3. S. Feher, **"HFDM 05 Test Summary Report"**, Fermilab note, TD-05-031.
4. V.V. Kashikhin, A.V. Zlobin, "**Magnetic Instabilities in Nb_3Sn Strands and Cables"**, *IEEE Transactions on Applied Superconductivity, Vol. 15, No. 2, June 2005, pp.1621-1624*.
5. G. Sabbi, S.E. Bartlett, S. Caspi, D.R. Dietderich, P. Ferracin, S.A. Gourlay, A.R. Hafalia, C.R. Hannaford, A.F. Lietzke, S. Mattafirri, A.D. McInturff, R. Scanlan, **"Design of HD2: A 15 Tesla Nb_3Sn Dipole With a 35 mm Bore"**, *IEEE Transactions on Applied Superconductivity, Vol. 15, No. 2, June 2005, pp.1128-1131*.